Wavelet-based vs. DCT-based Progressive Compression of Biological Specimens Images

V.G. Ruiz, J.J. Fernández, M.F. López, I. García *

Dept. Computer Architecture and Electronics
University of Almería.
04120 Almería. Spain.
E-mail: vruiz@ual.es, jose@ace.ual.es, jmflopez@ace.ual.es, inma@ace.ual.es
Tel: +34 950 015711

Abstract
This work presents a rigorous and objective evaluation of two progressive image transmission techniques in a framework of telemicroscopy of biological specimens. First of all, a Lossless Progressive Image Codec (LPIC) which is based on a specific wavelet transform and an efficient encoding method is introduced. This system is then compared to the standard Progressive-JPEG (P-JPEG) for the specific task of detecting biological specimens in the images progressively received by a biologist controlling a remote transmission electron microscope (TEM). Both methods have been quantitatively compared by means of a task-oriented methodology that guarantees an objective comparison. The results that have been obtained allow to claim with statistical significance that our method outperforms the standard P-JPEG throughout the transmission process.

Keywords
Discrete wavelet transform, progressive image transmission, SPIHT, JPEG, figures of merit in Telemicroscopy.

1 Introduction

Telemedicine, Telemicroscopy and Teleastronomy provide access to expensive and unique instruments for the scientific community, allowing one or several remote users to control devices in real time and/or to share the images obtained from the current experiment or to consult databases of images obtained from previous experiments. For these purposes, remote links must provide high rate transmission with short latencies in order to make the instrument available as a research tool. Apart from using a high transmission rate, a remote visualization procedure can be accelerated by using an appropriate image compressor. Most of the telemetry and remote control systems in Telemedicine, Teleastronomy or Telemicroscopy use the standard JPEG compressor/decompressor. The goal of this work is to describe and analyse a mechanism for

*This work has been partially supported by the Spanish CICYT through grants TIC99-0361 and TIC2002-00228.

the efficient transmission and lossless storage of the images, facilitating the remote operation of the TEM by the biologist. This mechanism basically consists of sending data images by a compressed and progressive way of transmission.

In this paper a Lossless Progressive Image Codec (LPIC) is proposed for this objective. Based on a rigorous methodology, the efficiency of the standard progressive compressor P-JPEG will be compared to LPIC for the specific task of searching and detecting biological specimens in the progressively sent images. In addition, a subjective visual comparison between both progressive compressors will also be provided. Subjective observations and numerical results obtained from an exhaustive analysis based on many experiments show that LPIC outperforms P-JPEG.

2 The Lossless Progressive Image Codec

Progressive image transmission systems are structured into two main blocks [1]. First, the transformation stage, which plays an important role in decorrelating and compacting image data by using a spectral decomposition. Second, a progressive-fidelity encoding stage, which is applied to the transform coefficients to create a compact code-stream in such a way that the image quality is gradually improved until a perfect reconstruction is obtained. In this work we have used a progressive image transmission system, called LPIC (Lossless Progressive Image Codec), which relies on a specific wavelet transform (13/7-T) [2] and an efficient codec (SPIHT, which stands for Set Partitioning In Hierarchical Trees) [3].

3 Methodology for Objective Comparison

LPIC and P-JPEG have been objectively evaluated by means of a task-oriented methodology which measures (via figures of merit) their performance according to the detectability of biological specimens in the images progressively transmitted. This methodology [4] consists of the following stages:

1. Generation of phantoms resembling real electron micrographs of fields with biological specimens.
2. Reconstruction of the image from the progressively transmitted images by the two methods to be compared.
3. Assignment of *figures of merit* (FOMs) to each reconstructed image.
4. Computation of the *statistical significance* (via a t-student test for paired data) at which the null hypothesis that the two methods perform equally well can be rejected in favour of that the method with higher average FOM is better for the specific task.
5. Computation of the *relevance* of the superiority of one of the methods over the other. This measure quantifies the importance of the improvements as
$$\frac{f_2 - f_1}{1 - f_1} \times 100\% \tag{1}$$
where f_1 and f_2 are the average values of the FOMs for the images reconstructed with the two methods.

Two types of phantoms resembling different types of electron micrographs commonly used in structural biology have been designed [5]: micrographs used in high resolution structural analyses of macromolecules and micrographs used in tomographic analyses at subcellular level.

Different levels of noise were included in the phantoms to resemble a wide spectrum of imaging conditions: the signal-to-noise ratio (SNR) was varied from 20 to 1.

A set of FOMs has been designed to measure the goodness of the image transmission method in reproducing the original image, with special emphasis in the biological specimens in it (the foreground). We have adapted and used the structural consistency FOMs commonly used in other fields (tomography). In addition, we have designed a new set of FOMs able to reflect the effect of the grey level quantization that occurs during the image transmission process. Finally, we have used a FOM based on the PSNR (Peak-SNR), a standard measure used in the image compression field.

To present the FOMs used in the experiments, we need to introduce some notation. We use r to denote the region (foreground, background or whole image) over which the FOM is measured; N_r represents the number of pixels inside the region r; $O_{r,i}$ is the scaled value of the pixel with index $i \in [1, N_r]$ in the region r of the original image, whereas $R_{r,i}$ is the corresponding one in the reconstructed image ($O_{r,i}$ and $R_{r,i}$ are scaled so that they range in [0,1]). Among many others, the three most representative FOMs that have been used in the evaluation are the following:

i) Mean squared error FOM

This FOM provides a structural consistency measure between pixel values in the original and reconstructed images.

$$scL2(r) = 1 - \frac{1}{N_r} \sum_{i=1}^{N_r} \left(\frac{O_{r,i} - R_{r,i}}{2} \right)^2 \tag{2}$$

ii) Entropy Difference FOM

This FOM is intended to quantify how well the reconstructed image is reproducing the average information in the original image, and is analytically defined as

$$hE(r) = 1 - \frac{|E_O(r) - E_R(r)|}{\log_2 L} \tag{3}$$

where L is the number of grey levels; r represents the region over which the FOM is measured; $E_O(r)$ and $E_R(r)$ denote the entropy of the original and reconstructed image, respectively. The entropy of an image I can be estimated from its histogram according to

$$E_I(r) = -\sum_{l=1}^{L} \frac{H_{I,r}(l)}{N_r} \log_2 \left(\frac{H_{I,r}(l)}{N_r} \right) \tag{4}$$

where $H_{I,r}(l)$, with $l = 1, \ldots, L$, denotes the histogram of the image I computed over the region r.

iii) PSNR FOM

The PSNR (stands for Peak Signal-to-Noise Ratio) metric is inversely proportional to the root mean squared error (RMSE). This standard metric has been adapted to consider the different regions of the image, so the formula of the PSNR FOM (in dB) is

$$\mathrm{PSNR}(r) = 10 \log_{10} \left(\frac{(2^p - 1)^2}{\mathrm{RMSE}(r)} \right) \tag{5}$$

where p denotes the number of bits/pixel, r represents the region in which the FOM is computed and $\mathrm{RMSE}(r)$ is

$$\mathrm{RMSE}(r) = \sum_{i=1}^{N_r} (O_{r,i} - R_{r,i})^2 \tag{6}$$

4 Experimental Results

4.1 Objective comparison based on phantoms

The objective comparison was performed over ensembles of the two types of phantoms. Fifty statistically independent phantoms were generated for every type. For each phantom, twenty additional noisy versions were generated, with SNR from 20 to 1. Therefore, two ensembles of 1050 synthetic images each were used to perform the objective comparison, which involves high levels of statistical significance.

Synthetic images were then progressively transmitted by means of the two methods: LPIC and P-JPEG (the latter with the maximum quality index: 100). The comparison was carried out at intervals of 0.1 bpp. The results of each FOM (measured for the foreground) are presented by a triad of graphs which exhibits the evolution as the transmission progresses: (1) The first graph is the mean value of the FOM. (2) The second graph represents the result of the significance testing. More specifically, those curves show the mean of the difference for paired data as well as the confidence interval at 95 % level. If such a mean is greater than 0.0, LPIC is, in average, performing better than P-JPEG for the specific task, at the corresponding bpp. A negative mean involves the opposite. (3) Finally, the third graph show the relevance of the superiority for the significance testing. Figs. 1, 2, and 3 show the results. Only the results for SNR=20 and SNR=1 are presented.

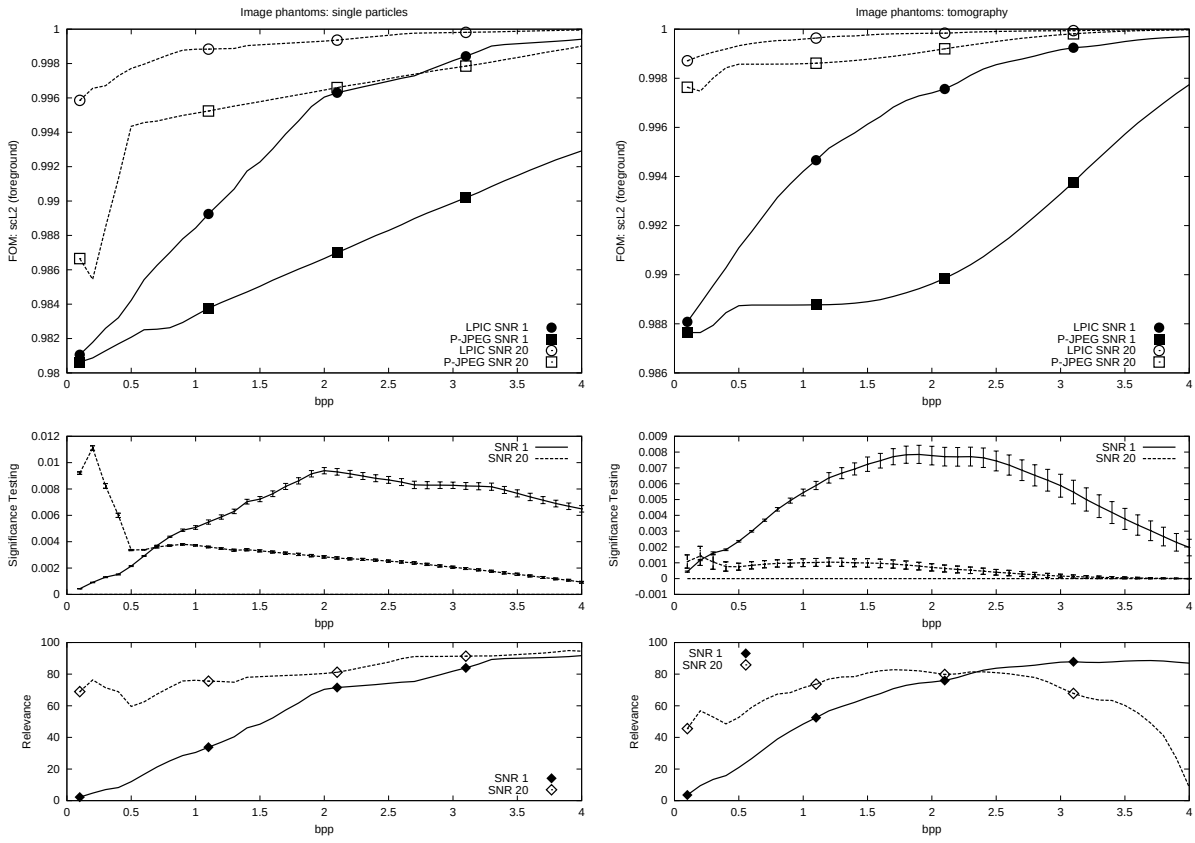

Figure 1: Results obtained for the scL2 FOM for the ensembles of single particle phantoms (left) and tomography phantoms (right).

An analysis of the results from a global perspective allows to draw interesting conclusions

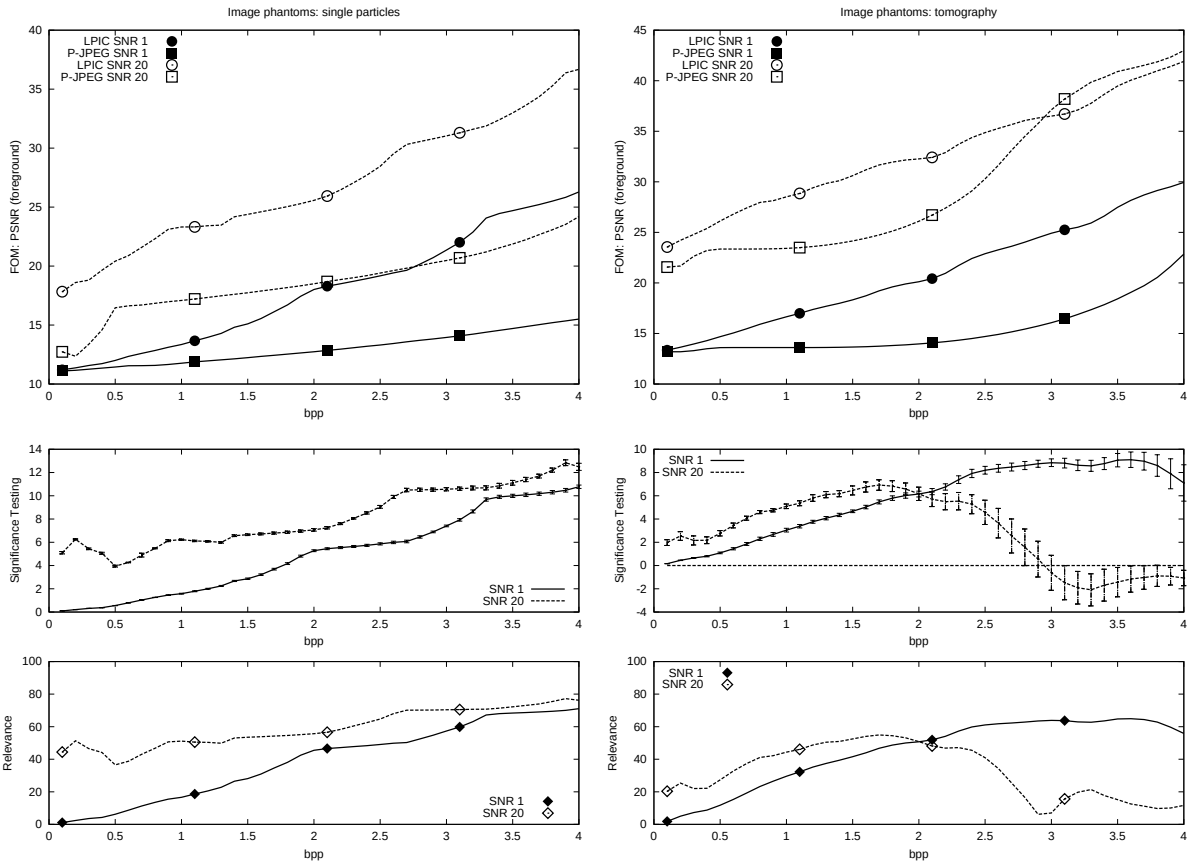

Figure 2: Results obtained for the PSNR FOM for the ensembles of single particle phantoms (left) and tomography phantoms (right).

about the general behaviour of both progressive image transmission methods:
1. P-JPEG systematically exhibits a drop in performance at the beginning of the transmission (around 0.1 - 0.5 bpp) compared to its general behaviour thereinafter. This drop takes place for most of the FOMs, for both types of phantoms and for all of the SNRs. We speculate that this fact may be caused by the severe blocking artifacts that P-JPEG undergoes at the beginning of the transmission.
2. In general, LPIC exhibits a positive slope much greater than P-JPEG at the first stages of the transmission (0.1 - 2 bpp). This causes that LPIC leads the transmission from the beginning and P-JPEG then progresses to reach for LPIC around the middle or the end (depending on the FOM) of the transmission. This conclusion is guaranteed by the fact that the confidence intervals for the paired difference prove to be very tight. This leading position of LPIC is caused by the logarithm-like curves which, in general, LPIC describes and that asymptotically reach 1.0, the maximum FOM value. On the contrary, P-JPEG describes sigmoidal-like or linear-like curves (from 0.5 bpp on) that approach 1.0.
3. According to scL2 and PSNR FOMs, LPIC and P-JPEG perform equally well at the beginning of the transmission for extremely low SNRs. Nevertheless, from the visual point of view, LPIC is better than P-JPEG at those ranges of bpp, as will be shown later. In such situations, the FOM hE works much better since it quantitatively reflects the visual differences between the methods from the beginning.
4. In general, we can state that, for the task of the detection of biological specimens in progressive transmitted images in telemicroscopy, LPIC outperforms P-JPEG. This assertion is guaranteed

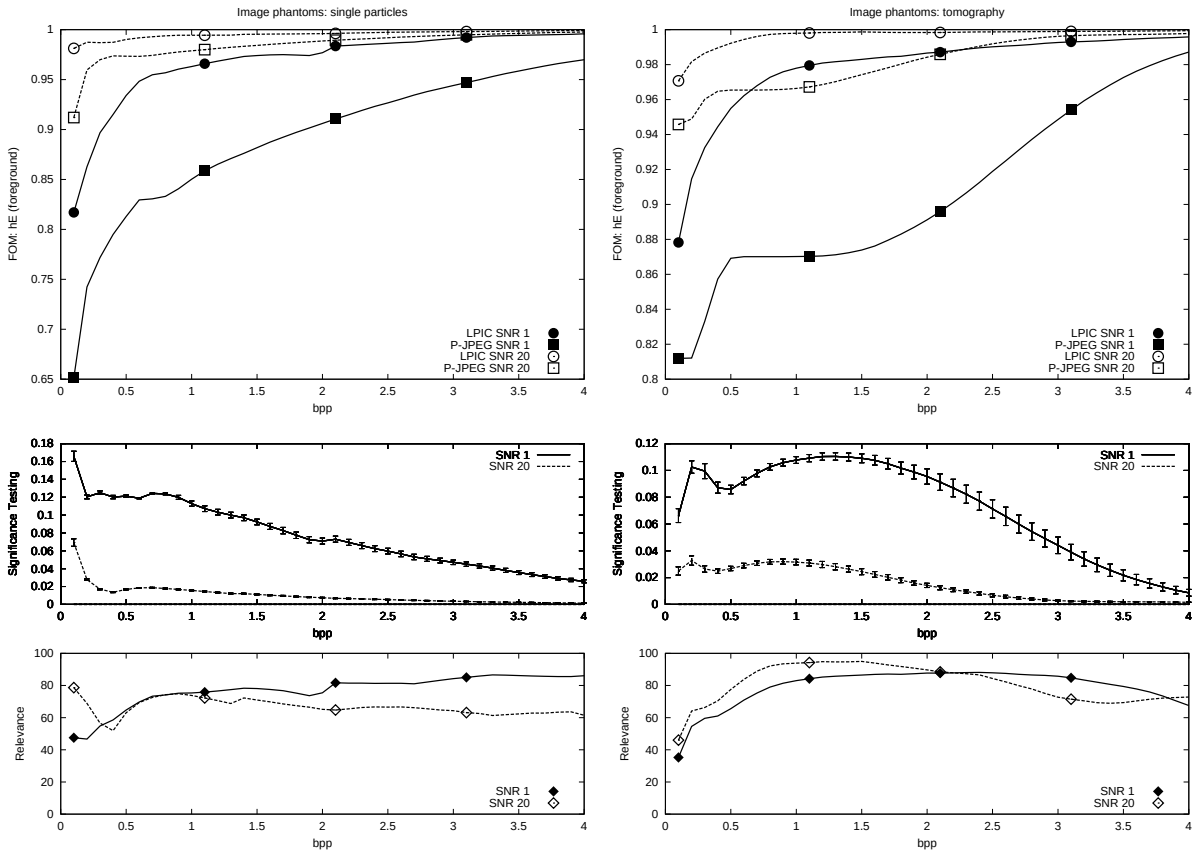

Figure 3: Results obtained for the hE FOM for the ensembles of single particle phantoms (left) and tomography phantoms (right).

by the rigorous analysis based on the task-oriented objective comparison methodology.

4.2 Evaluation based on real images

The progressive image transmission methods were also evaluated in their application to experimental conditions. Both, LPIC and P-JPEG, were applied and evaluated on a set of real TEM images of biological specimens. For these images, all the FOMs were computed, and the exhibited behaviour has turned out to be very similar to that presented for the phantoms (curves not shown here).

Finally, in this work we also intend to show the quality of the progressive transmission for real images from the visual point of view. The attention is centered on the beginning of the transmission, where the strongest artifacts arise in the reconstructed images. The results of reconstructing an experimental image at only 0.1 bpp are shown in Figure 4. At the upper left, an experimental image of transmissible gastroenteritis coronavirus is shown. A zoomed area is shown at the upper right of the figure. The LPIC reconstructed image from 0.1 bpp is shown in the middle left, together with the detailed area at the right. Finally, the P-JPEG reconstructed image at 0.1 bpp and the corresponding zoomed area are shown at the bottom. From Figure 4 it can be clearly appreciated that the image reconstructed by P-JPEG undergoes severe blurring and blocking artifacts compared to LPIC. Furthermore, as P-JPEG works in multiple line-scans, at the very beginning of the transmission there are rows with no image information to display, as shown in Figure 4. The image that LPIC reconstructs at 0.1 bpp exhibits much more contrast

and even structural details at local level.

5 Conclusion

The thorough objective evaluation allows to claim that LPIC clearly outperforms P-JPEG during the whole transmission process for both types of images and for the whole range of signal-to-noise ratios. More specifically, the superiority of LPIC is evident at the beginning of the transmission (up to 0.5 bpp), which is the range where the strongest visual artifacts arise in the reconstructed images. Similar behaviour has been obtained with experimental data. Furthermore, the fact that LPIC is a lossless image compressor method ensures that the image that finally is received at the end of the transmission is an exact replica of the original one.

Visualization results have shown the superiority in quality of LPIC over P-JPEG. LPIC exhibits excellent levels of details from the very beginning and, moreover, it does not experience the severe blocking artifacts that P-JPEG undergoes at the first stages of the transmission.

References

[1] M.F. López, V.G. Ruiz, J.J. Fernández, and I. García, "Progressive-Fidelity Image Transmission for Telebrowsing: An Efficient Implementation," in *Proc. IASTED International Conference on Visualization, Imaging and Image Processing*, 2001, pp. 334–339.

[2] D.A. Adams and F. Kossentini, "Reversible Integer-to-Integer Wavelet Transforms for Image Compression: Performance Evaluation and Analysis," *IEEE Trans. Image Proc.*, vol. 9, pp. 1010–1024, 2000.

[3] A. Said and W.A. Pearlman, "A New, Fast, and Efficient Image Codec Based on Set Partitioning in Hierarchical Trees," *IEEE Trans. Cir. Sys. Vid. Tec.*, vol. 6, pp. 243–250, 1996.

[4] S.S. Furuie, G.T. Herman, T.K. Narayan, P.E. Kinahan, J.S. Karp, R.M. Lewitt, and S. Matej, "A methodology for testing statistically significant differences between fully 3D PET reconstruction algorithms," *Phys. Med. Biol.*, vol. 39, pp. 341–354, 1994.

[5] J. Frank, *Three Dimensional Electron Microscopy of Macromolecular Assemblies*, Academic Press, 1996.

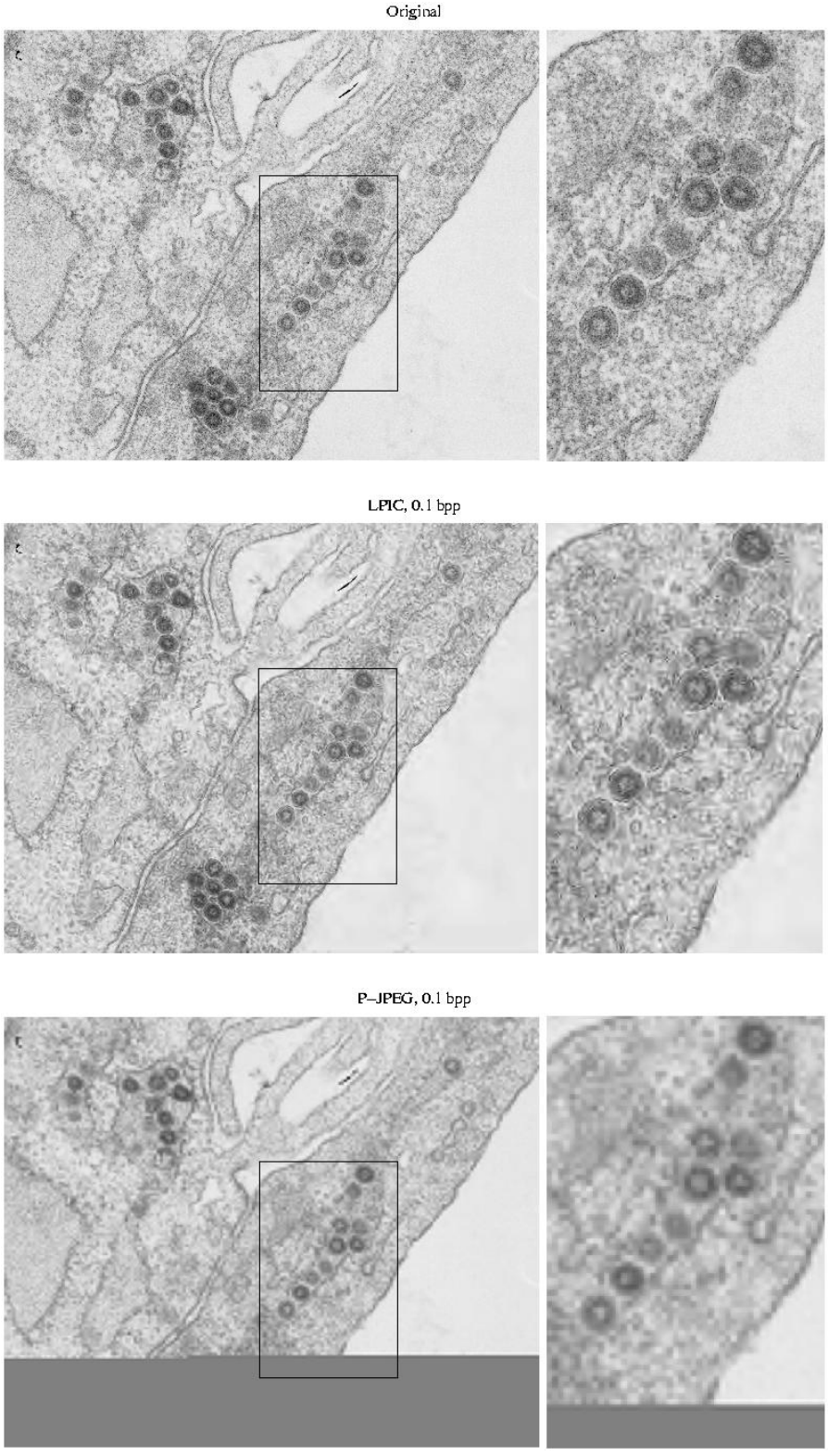

Figure 4: Visualization of the reconstruction at 0.1 bpp of an image of transmissible gastroenteritis coronavirus.